

Thermoelectric properties of delafossite-type layered oxides $\text{AgIn}_{1-x}\text{Sn}_x\text{O}_2$

Masahiro Yasukawa^{a)} and Kaoru Ikeuchi

Department of Materials Science and Engineering, Kochi National College of Technology,
200-1 Monobe, Nankoku 783-8508, Japan

Toshio Kono

Kochi Prefectural Industrial Technology Center, 3992-3 Numoshida, Kochi 781-5101, Japan

Kazushige Ueda

Department of Materials Science, Faculty of Engineering, Kyushu Institute of Technology,
1-1 Sensui, Tobata, Kitakyushu 804-8550, Japan

Hideo Hosono

Materials and Structures Laboratory, Tokyo Institute of Technology, 4259 Nagatsuta,
Midori, Yokohama 226-8503, Japan

(Received 17 January 2005; accepted 29 April 2005; published online 6 July 2005)

The thermoelectric properties of delafossite-type layered oxides $\text{AgIn}_{1-x}\text{Sn}_x\text{O}_2$ that consist of alternating layers of Ag and $\text{In}_{1-x}\text{Sn}_x\text{O}_2$ were investigated to elucidate their potential as a thermoelectric material. Polycrystalline materials of the $\text{AgIn}_{1-x}\text{Sn}_x\text{O}_2$ were prepared by a cation exchange reaction between $\text{NaIn}_{1-x}\text{Sn}_x\text{O}_2$ and AgCl . The solubility limit of the Sn atoms on the In sites was approximately $x=0.05$. The electrical conductivity and Seebeck coefficient were measured between 373 and 673 K in air. Undoped AgInO_2 was an *n*-type semiconductor with conductivities of 10^{-4} – $10^{-2} \Omega^{-1} \text{cm}^{-1}$, and the electron carriers were generated via the formation of oxygen vacancies. $\text{AgIn}_{0.95}\text{Sn}_{0.05}\text{O}_2$ was an *n*-type degenerate semiconductor with conductivities of 10^0 – $10^1 \Omega^{-1} \text{cm}^{-1}$ where the Sn atoms acted as electron donors. This drastic increase in the electrical conductivity increased the thermoelectric power factor by approximately two orders of magnitude to 10^{-6} – $10^{-5} \text{W m}^{-1} \text{K}^{-2}$. © 2005 American Institute of Physics.

[DOI: 10.1063/1.1940133]

I. INTRODUCTION

Thermoelectric energy conversion is an important technology for utilizing clean energy and development of thermoelectric materials with high efficiency of energy conversion is a key issue. Low-dimensional materials that consist of conducting one-dimensional (1D) chains or two-dimensional (2D) layers are promising for thermoelectric energy conversion.^{1–4} One advantage of the low dimensionality proposed in these papers can be interpreted in terms of the carrier confinement effect in the conducting 1D chains or 2D layers, which leads to an enlarged absolute value of the Seebeck coefficient *S* compared to the materials with three-dimensional conducting paths. Another advantage is a phonon-scattering effect due to the different chemical bonding between the chains or layers, which decreases the thermal conductivity κ . In addition, the electrical conductivity σ of the low-dimensional materials can also be controlled by doping on the sublattice outside of the conducting paths to prevent the carrier mobility from decreasing. These three advantages are promising for a high thermoelectric figure of merit *Z* expressed by the equation $Z=S^2\sigma/\kappa$, although there may be some trade-offs between the advantages.

Delafossite-type oxides are layered materials that consist of a variety of compositions expressed by the general formula ABO_2 (*A*=Pt, Pd, Cu, and Ag; *B*=Al, Ga, In, Sc, Cr,

Fe, Co, Y, La, etc.).^{5–7} The crystal structure consists of an alternating stacks of the A^+ layer and the $(\text{BO}_2)^-$ layer along the *c* axis. There are two polytypes, rhombohedral (3*R*) and hexagonal (2*H*), according to the stacking sequence of a unit of the A^+ and $(\text{BO}_2)^-$ layers.⁸ The 3*R* type has a stacking sequence of *abcabc*···, where each of *a*, *b*, and *c* denotes a unit of the A^+ and $(\text{BO}_2)^-$ layers as shown in Fig. 1. The A^+ cations form linear O–A–O dumbbells parallel to the *c* axis and the $(\text{BO}_2)^-$ layers form sheets with edge-sharing BO_6 octahedra. The O atom coordinated by one *A* atom and three

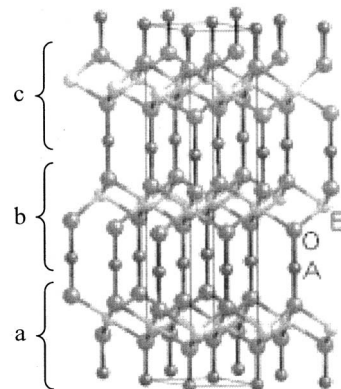


FIG. 1. Crystal structure of delafossite-type ABO_2 (space group: $R\bar{3}m$). The structure has a stacking sequence of *abcabc*··· along the *c* axis, where each of *a*, *b*, and *c* denotes a unit of the A^+ and $(\text{BO}_2)^-$ layers. The solid line shows the trigonal unit cell.

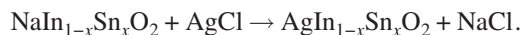
^{a)}Author to whom correspondence should be addressed; electronic mail: yasukawa@ms.kochi-ct.ac.jp

B atoms has a sp^3 -like bonding configuration. When the A^+ cation is monovalent Pt or Pd with a d^9 electronic configuration, the materials show a metallic conductivity, whereas the materials are semiconductors with monovalent Cu or Ag with d^{10} closed shells.^{5–7} For the latter, transparent conducting thin films with both *p*-type and *n*-type conductivities are extensively developed based on the unique material design concept.^{9–13} Koumoto and co-workers^{4,14} reported the thermoelectric properties of several delafossite-type oxides, polycrystalline materials of $PdCoO_2$ and Ag_xCoO_2 , and a single crystal of $CuAlO_2$ at high temperatures. They found that the $PdCoO_2$ and $CuAlO_2$ are promising thermoelectric materials that display a *p*-type conductivity.

We have selected a delafossite-type layered oxide $AgInO_2$ as a candidate of thermoelectric material. Transparent thin films of Sn-doped $AgInO_2$ with an *n*-type conductivity were fabricated by a rf-sputtering method¹² and a pulsed laser deposition method.¹³ In these studies, the electrical conductivity was successfully controlled by Sn doping and the conducting paths for the electron carriers were considered to be InO_2 layers. In this study, polycrystalline bulk materials of $AgIn_{1-x}Sn_xO_2$ have been prepared by a cation exchange reaction and the thermoelectric properties have been investigated at high temperatures. The effect of Sn doping on the thermoelectric power factor is reported.

II. EXPERIMENT

Since it is known that the direct preparation of $AgInO_2$ delafossite by a conventional solid-state reaction of In_2O_3 with $AgNO_3$ or Ag_2O was unsuccessful,¹² powder samples of delafossite-type $AgIn_{1-x}Sn_xO_2$ with $x=0.00$, 0.05, and 0.10 were prepared by a cation exchange reaction between $NaIn_{1-x}Sn_xO_2$ and $AgCl$. The starting materials, Na_2CO_3 , In_2O_3 , and SnO_2 , were stoichiometrically weighed and mixed in ethanol. The mixed powder was pressed into a pellet, which was heated and intermittently ground at 1123 K for 20 h in air flow. The obtained $NaIn_{1-x}Sn_xO_2$ was ground and stoichiometrically mixed with $AgCl$ in a mortar. The mixed powder was pressed into a pellet and the following cation exchange reaction was performed by heating at 673 K for 24 h in air with intermittent grinding:



The pulverized sample was washed in distilled water, filtered, and dried at 353 K in air. Then the sample was pressed into a cylinder at 200 MPa using a cold isostatic press. Afterwards, it was heated at 673 K for 12 h in air. A phase identification was performed by x-ray-powder-diffraction (XRD) measurements using $Cu K\alpha$ radiation (PANalytical, X'Pert). The electrical conductivity and Seebeck coefficient were measured at several temperatures between 373 and 673 K in air using an equipment developed in our laboratory. The electrical conductivity was measured by the direct current four-probe method. The Seebeck coefficient was evaluated by correcting the linear gradient of $\Delta V/\Delta T$ for the thermopower of platinum,¹⁵ where ΔV and ΔT are the thermoelectromotive force and the temperature difference between both ends of a sample measured by Pt leads and

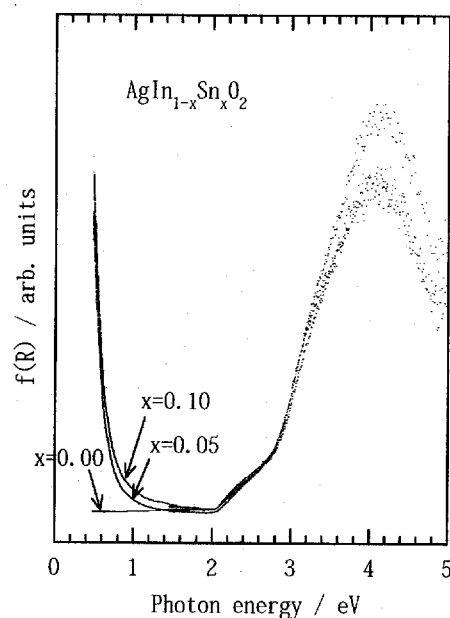


FIG. 2. Kubelka–Munk function spectra for $AgIn_{1-x}Sn_xO_2$ ($x=0.00$, 0.05, and 0.10). The spectra were obtained by transforming the diffuse reflectance spectra measured for the powder samples. MgO powder was used as a reference.

Pt/Pt – Rh thermocouples, respectively. Diffuse reflectance spectra were measured in a wavelength range of 200–2600 nm for the powder samples using double-beam spectrophotometer (Hitachi, U-4000). MgO powder was used as a reference. The Kubelka–Munk function spectra were obtained using the equation $f(R)=(1-R)^2/2R$, where $f(R)$ is the Kubelka–Munk function and R is the diffuse reflectance.

III. RESULTS AND DISCUSSION

The XRD patterns for the samples with $x=0.00$ and 0.05 were indexed with a $3R$ -type delafossite structure of $AgInO_2$,¹⁶ indicating that the obtained samples with $x=0.00$ and 0.05 were single phases of the delafossite-type $AgIn_{1-x}Sn_xO_2$. The XRD pattern for the sample with $x=0.10$ showed a few weak diffraction peaks besides those arising from the $3R$ -type delafossite, which were due to $AgCl$ and probably Sn-related oxide impurity. This result suggests that the solubility limit of the Sn atoms into the In site is approximately $x=0.05$ at the preparation stage of the precursor $NaIn_{1-x}Sn_xO_2$. Significant differences in the lattice parameters a and c of the $3R$ -type delafossite structure were not observed among the samples: $a=3.2764(2)$ Å, $c=18.875(3)$ Å for $x=0.00$, $a=3.2759(2)$ Å, $c=18.879(2)$ Å for $x=0.05$, and $a=3.2755(2)$ Å, $c=18.879(2)$ Å for $x=0.10$, respectively. These values are consistent with those previously reported for $AgInO_2$.^{5,16,17} Using the theoretical relative densities calculated from the lattice parameters, the estimated relative densities of the cylindrical samples were approximately 60%. Although the sample with $x=0.10$ included a small amount of impurities, the optical and thermoelectric measurements were performed for comparison.

Figure 2 shows the Kubelka–Munk function spectra. A

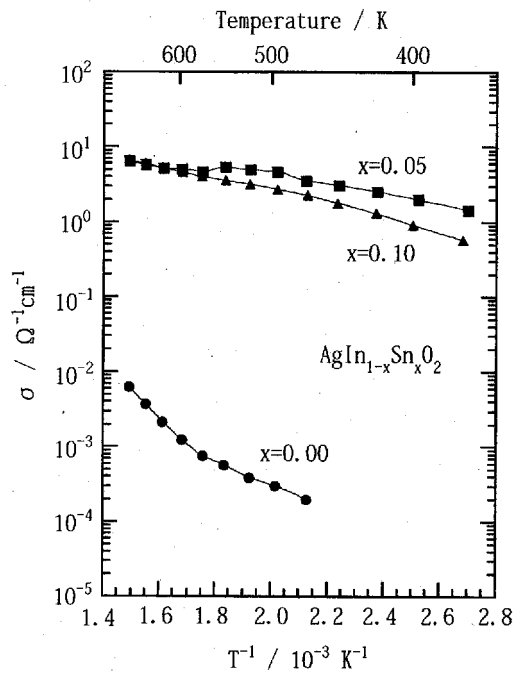


FIG. 3. Temperature dependence of the electrical conductivity σ for $\text{AgIn}_{1-x}\text{Sn}_x\text{O}_2$ ($x=0.00, 0.05$, and 0.10).

weak optical absorption starts at a photon energy of 2.05 eV and a sharp increase in the absorption is observed at approximately 3 eV for all the samples. These two optical absorptions correspond to the indirect and direct band gaps of the delafossite-type $\text{AgIn}_{1-x}\text{Sn}_x\text{O}_2$, respectively.^{13,18} Another optical absorption is observed in the lower photon energy side for the Sn-doped samples. This absorption is attributed to the plasma oscillation of electron carriers generated from the doped Sn atoms¹³ and indicates that the doped Sn atoms act effectively as electron donors.

Figure 3 shows the temperature dependence of the electrical conductivity. The electrical conductivity for the undoped AgInO_2 is 10^{-4} – 10^{-2} $\Omega^{-1}\text{cm}^{-1}$ between 473 and 673 K, and the value increases as the temperature increases. The 5-mol % Sn doping drastically enhanced the electrical conductivity to 10^0 – 10^1 $\Omega^{-1}\text{cm}^{-1}$, which is more than three orders of magnitude higher than that of undoped AgInO_2 . This enhanced electrical conductivity was also demonstrated for 5-mol % Sn-doped AgInO_2 thin film.¹² Figure 4 shows the temperature dependence of the Seebeck coefficient. The signs of the Seebeck coefficient are negative for all the samples, indicating that the materials are *n*-type conductors. The absolute value of the Seebeck coefficient for the undoped AgInO_2 decreases with increasing temperature, suggesting the increase in the electron carriers with the temperature increase. The absolute value of the Seebeck coefficient drastically decreases with 5-mol % Sn doping, corresponding to the effective electron doping, but it remains higher than 100 $\mu\text{V K}^{-1}$ at 673 K.

The observed thermoelectric properties suggest that the undoped AgInO_2 is an *n*-type semiconductor, and the electron carriers are probably generated from the oxygen vacancies according to the following defect equilibrium using the Kröger–Vink notation:

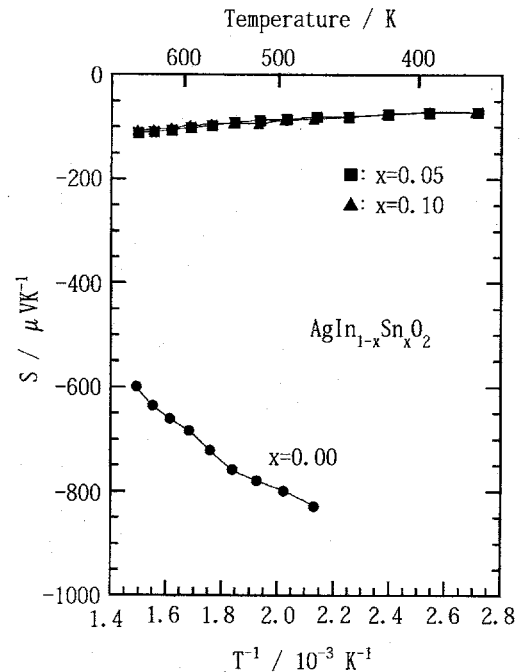
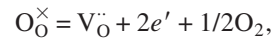


FIG. 4. Temperature dependence of the Seebeck coefficient S for $\text{AgIn}_{1-x}\text{Sn}_x\text{O}_2$ ($x=0.00, 0.05$, and 0.10).



where O_O , V_O , and e are the O^{2-} anion in the delafossite lattice, the oxygen vacancy, and electron carrier, respectively, and the superscripts \times , \cdot , and $'$ denote effective charge states of neutral, positive, and negative, respectively. It is likely that the oxygen vacancy releasing two electrons as electron donor increases as the temperature increases. For the Sn-doped sample with $x=0.05$, the conductivity gradually increases and the absolute value of the Seebeck coefficient linearly increases as the temperature increases. These behaviors suggest that the $\text{AgIn}_{0.95}\text{Sn}_{0.05}\text{O}_2$ is a degenerate semiconductor and the Sn atoms doped in the delafossite lattice act effectively as electron donors, being consistent with the optical absorption by the electron carriers. There are no significant differences in the electrical conductivity and Seebeck coefficient between the Sn-doped samples with $x=0.05$ and 0.10 . This is consistent with the XRD result that the solubility limit of the Sn atoms into the In site is approximately $x=0.05$ and suggests that a small amount of impurities in the sample with $x=0.10$ hardly affect the thermoelectric properties. Rogers *et al.*⁷ explained the electrical transport properties of the delafossite-type oxides using a molecular-orbital energy diagram and the hybridization between d_{z^2} and s orbitals proposed by Orgel.¹⁹ Their explanation indicated that the valence band of the materials is composed of filled d_{z^2} – s hybrid orbitals or other nonhybrid d orbitals that directly interact with the corresponding orbitals of the neighboring Ag^+ cations in the c plane due to the relatively short distance between the Ag^+ cations [3.2772 Å for AgInO_2 (Ref. 5)] and that the lower part of the conduction band is composed of empty antibonding orbitals be-

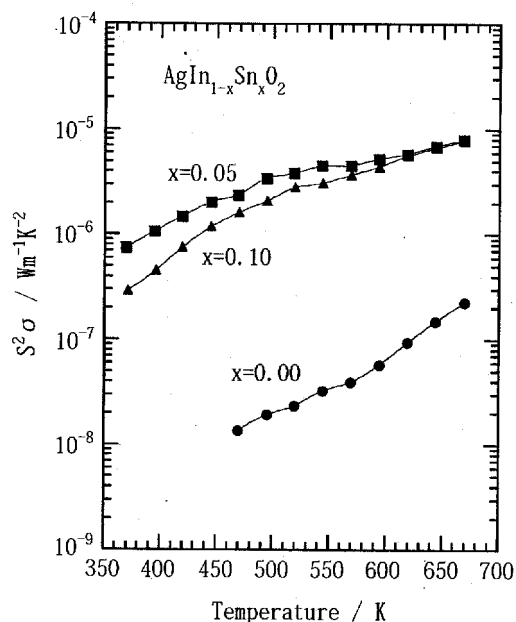


FIG. 5. Temperature dependence of the thermoelectric power factor $S^2 \sigma$ for $\text{AgIn}_{1-x}\text{Sn}_x\text{O}_2$ ($x=0.00, 0.05,$ and 0.10).

tween the Ag d_{z^2+s} hybrid orbitals and the O sp^3 hybrid orbitals along the c axis. For AgInO_2 , the lowest part of the conduction band may be composed of antibonding orbitals between the In $5s$ and O sp^3 orbitals. Therefore, the electron carriers generated from the doped Sn atoms and the oxygen vacancies will move through the InO_2 layers, as described in the previous paper.¹³

Figure 5 shows the temperature dependence of the thermoelectric power factor. The power factor values for undoped AgInO_2 are 10^{-8} – 10^{-7} $\text{W m}^{-1} \text{K}^{-2}$ between 470 and 670 K, but 5-mol % Sn doping drastically enhanced the values to 10^{-6} – 10^{-5} $\text{W m}^{-1} \text{K}^{-2}$ between 370 and 670 K. The power factor also increases with increasing temperature for all the samples. Since the relative densities of the present samples that had the electrical conductivity and Seebeck coefficient measured are still low ($\sim 60\%$), improving the relative density using an effective technique of ceramic processing or thin film preparation is considered the key to further increasing the electrical conductivity and, consequently, the power factor. Thus, $\text{AgIn}_{1-x}\text{Sn}_x\text{O}_2$ is a promising n -type thermoelectric material.

IV. CONCLUSIONS

Delafossite-type layered oxides $\text{AgIn}_{1-x}\text{Sn}_x\text{O}_2$ were prepared by a cation exchange reaction and the thermoelectric properties were investigated between 370 and 670 K.

- (1) The solubility limit of the Sn atoms on the In sites is approximately $x=0.05$ in the present synthesis route.
- (2) Undoped AgInO_2 is an n -type semiconductor in which electron carriers are generated via the formation of oxygen vacancies, whereas the Sn-doped material of $\text{AgIn}_{0.95}\text{Sn}_{0.05}\text{O}_2$ is an n -type degenerate semiconductor where the doped Sn atoms effectively act as electron donors.
- (3) The optical absorption due to the electron carriers is clearly observed in the near-infrared wavelength region for the $\text{AgIn}_{0.95}\text{Sn}_{0.05}\text{O}_2$.
- (4) The electrical conductivity is drastically enhanced with 5-mol % Sn doping and increases the thermoelectric power factor by approximately two orders of magnitude to 10^{-6} – 10^{-5} $\text{W m}^{-1} \text{K}^{-2}$.

ACKNOWLEDGMENTS

This work is a Collaborative Research Project of Materials and Structures Laboratory, Tokyo Institute of Technology and is partly supported by the Nippon Sheet Glass Foundation for Materials Science and Engineering.

- ¹L. D. Hicks and M. S. Dresselhaus, Phys. Rev. B **47**, 12727 (1993).
- ²L. D. Hicks and M. S. Dresselhaus, Phys. Rev. B **47**, 16631 (1993).
- ³R. Venkatasubramanian, E. Siivola, T. Colpitts, and B. O'Quinn, Nature (London) **413**, 597 (2001).
- ⁴K. Koumoto, H. Koduka, and W.-S. Seo, J. Mater. Chem. **11**, 251 (2001).
- ⁵R. D. Shannon, D. B. Rogers, and C. T. Prewitt, Inorg. Chem. **10**, 713 (1971).
- ⁶C. T. Prewitt, R. D. Shannon, and D. B. Rogers, Inorg. Chem. **10**, 719 (1971).
- ⁷D. B. Rogers, R. D. Shannon, C. T. Prewitt, and J. L. Gillson, Inorg. Chem. **10**, 723 (1971).
- ⁸J.-P. Doumerc, A. Ammar, A. Wichainchai, M. Pouchard, and P. Hagenmuller, J. Phys. Chem. Solids **48**, 37 (1987).
- ⁹H. Kawazoe, M. Yasukawa, H. Hyodo, M. Kurita, H. Yanagi, and H. Hosono, Nature (London) **389**, 939 (1997).
- ¹⁰H. Kawazoe and K. Ueda, J. Am. Ceram. Soc. **82**, 3330 (1999).
- ¹¹H. Yanagi, H. Kawazoe, A. Kudo, M. Yasukawa, and H. Hosono, J. Electroceram. **4**, 407 (2000).
- ¹²T. Otabe, K. Ueda, A. Kudoh, H. Hosono, and H. Kawazoe, Appl. Phys. Lett. **72**, 1036 (1998).
- ¹³S. Ibuki, H. Yanagi, K. Ueda, H. Kawazoe, and H. Hosono, J. Appl. Phys. **88**, 3067 (2000).
- ¹⁴H. Yagi, W.-S. Seo, and K. Koumoto, Key Eng. Mater. **181–182**, 63 (2000).
- ¹⁵N. Cusack and P. Kendall, Proc. Phys. Soc. London **72**, 898 (1958).
- ¹⁶B. U. Köehler and M. Jansen, J. Solid State Chem. **71**, 566 (1987).
- ¹⁷D. Y. Shahriari, N. Erdman, U. T. M. Haug, M. C. Zarzychny, L. D. Marks, and K. R. Poeppelmeier, J. Phys. Chem. Solids **64**, 1437 (2003).
- ¹⁸H. Yanagi, S. Inoue, K. Ueda, H. Kawazoe, H. Hosono, and N. Hamada, J. Appl. Phys. **88**, 4159 (2000).
- ¹⁹L. E. Orgel, J. Chem. Soc. 4186 (1958).